第 29 卷 第 10 期　　催 化 学 报　　2008 年 10 月
Vol. 29 No. 10　　*Chinese Journal of Catalysis*　　October 2008

文章编号：0253-9837(2008)10-1043-08　　研究论文：1043～1050

负载型 CeO_2-ZrO_2 固溶体的性能及其在甲烷燃烧 Pd 催化剂中的应用

王晓红[1,2]，卢冠忠[1]，郭　耘[1]，乔东升[1]，张志刚[1]，郭杨龙[1]，李春忠[2]

（1 华东理工大学工业催化研究所结构可控先进功能材料及其制备教育部重点实验室，上海 200237；
2 华东理工大学超细材料制备与应用教育部重点实验室，上海 200237）

摘要：以硅改性的氧化铝为载体，用反相微乳液法合成了负载型的 CeO_2-ZrO_2 固溶体（Ce-Zr-O/Si-Al_2O_3），用低温氮吸附、X 射线衍射、程序升温还原、拉曼光谱和 X 射线光电子能谱等方法对 Ce-Zr-O/Si-Al_2O_3 的织构性能、热稳定性和储放氧性能等进行了表征. 结果表明，负载后的 CeO_2-ZrO_2 晶相与负载前相比没有变化，但热稳定性和在低温下的放氧能力及总储氧量明显提高. 作为甲烷燃烧 Pd 催化剂的载体，Ce-Zr-O/Si-Al_2O_3 的性能明显优于 CeO_2-ZrO_2，Si-Al_2O_3 和机械混合物 CeO_2-ZrO_2 + Si-Al_2O_3. 使用 0.2%Pd/10%Ce-Zr-O/Si-Al_2O_3 为催化剂时，甲烷 90%转化率时的温度仅为 345 ℃，比负载在其它载体上的 Pd 催化剂低 175 ℃.

关键词：负载型氧化铈-二氧化锆固溶体；硅改性氧化铝；钯催化剂；催化活性；甲烷燃烧

中图分类号：O643　　**文献标识码**：A

Properties of CeO_2-ZrO_2 Solid Solution Supported on Si-Modified Alumina and Its Application in Pd Catalyst for Methane Combustion

WANG Xiaohong[1,2], LU Guanzhong[1*], GUO Yun[1], QIAO Dongsheng[1], ZHANG Zhigang[1], GUO Yanglong[1], LI Chunzhong[2]

(*1 Laboratory for Advanced Materials, Research Institute of Industrial Catalysis, East China University of Science and Technology, Shanghai 200237, China; 2 Key Laboratory for Ultrafine Materials of Ministry of Education, East China University of Science and Technology, Shanghai 200237, China*)

Abstract: CeO_2-ZrO_2 solid solution was supported on Si-modified alumina (Ce-Zr-O/Si-Al_2O_3) by the reverse microemulsion method. Its structure, thermal stability, and oxygen release capacity were studied by N_2 adsorption, XRD, TPR, Raman spectroscopy, and XPS. The crystalline phase of Ce-Zr-O on Si-Al_2O_3 was the same as that of unsupported CeO_2-ZrO_2 (Ce-Zr-O), but its thermal stability, oxygen release capacity at low temperature, and total oxygen storage capacity were higher. As the support of a Pd catalyst for methane combustion, Ce-Zr-O/Si-Al_2O_3 had better properties than Ce-Zr-O, Si-Al_2O_3, and the mixture of Ce-Zr-O + Si-Al_2O_3. Using the 0.2%Pd/10%Ce-Zr-O/Si-Al_2O_3 catalyst, T_{90} for methane combustion was only 345 ℃, which was 175 ℃ lower than that of Pd supported on other supports.

Key words: supported ceria-zirconia solid solution; silicon-modified alumina; palladium catalyst; catalytic activity; methane combustion

Received date: 1 August 2008.

* **Corresponding author.** Fax: +86-21-64253703; E-mail: gzhlu@ecust.edu.cn

Foundation item: Supported by the National Basic Research Program of China (2004CB719500), the National Natural Science Foundation of China (20601008), and the Commission of Science and Technology of Shanghai Municipality (06 JC14095).

English edition available online at ScienceDirect (http://www.sciencedirect.com/science/journal/18722067).

It is well known that alumina and CeO_2-ZrO_2 solid solution are two important materials for three-way catalysts (TWCs) and VOCs (volatile organic compounds) combustion catalysts[1-5]. Alumina plays the role of a support, and CeO_2-ZrO_2 solid solution plays the role of a promoter. Generally, these two components are prepared individually and then mixed in the catalyst. As the support of catalysts used at high temperatures in reactions such as catalytic combustion of hydrocarbons and catalytic purification for the exhaust of vehicles, alumina should have high thermal stability because the high temperature can cause activity loss by both structural change (transformation of transition alumina to corundum) and textural change (loss of surface area and porosity). Therefore, increasing the thermal stability of alumina is of primary industrial interest. The stability of alumina can be promoted by doping it with elements such as alkaline earth metals, rare-earth metals[6], and silicon[7-9], and by improving the synthesis method, or by a combination of the two[7-13]. As a promoter of TWCs, CeO_2-ZrO_2 solid solution acts as an "oxygen buffer" by reduction/oxidation cycles between Ce^{4+} and Ce^{3+}[14], which stabilizes the dispersion of precious metals and the alumina support[15], promotes water-gas shift and steam reforming reactions[16], and suppresses the strong interaction between the precious metals and alumina[17]. As an oxygen storage material, CeO_2-ZrO_2 solid solution must possess a single phase, high thermal stability of the structure, and good textural (such as a high surface area) and oxygen handling properties (such as high reducibility). To achieve high performance of CeO_2-ZrO_2, nanostructured CeO_2-ZrO_2 solid solutions were prepared by using an appropriate design and doping with other elements[18-20].

Because the alumina support has a high surface area and can maintain the high dispersion of active PdO_x to achieve an effective utilization of precious metals, and the synergistic action between Ce-Zr-O and PdO can lead to high catalytic activity and thermal stability of the precious metal catalysts for the combustion of VOCs, a question is whether we can design and prepare a material with the advantages of Ce-Zr-O and alumina. On the basis of our studies on high thermal stability alumina and CeO_2-ZrO_2 solid solution[21-24], a CeO_2-ZrO_2 solid solution supported on Si-modified alumina was prepared and its physicochemical properties were characterized. It was an excellent support material for a Pd catalyst to catalyze methane combustion.

1 Experimental

1.1 Catalyst preparation

The preparation of CeO_2-ZrO_2 solid solution supported on Si-modified alumina included two steps. The first step was the preparation of Si-modified alumina, which was the same as in Ref. [21]. Polyethylene glycol octylphenyl ether (CR) was used as the surfactant, cyclohexane (AR) as the oil phase, and 1-hexanol (CR) as the co-surfactant. Water, surfactant, cosurfactant, and oil phases (volume ratio of 1.5∶1∶1.2∶7.2) were mixed, and this mixture was divided into two parts. A 1 mol/L aluminum nitrate (AR) aqueous solution (with a suitable amount of tetraethyl orthosilicate) was slowly added to one part of the mixture solution under stirring until a clear and one-phase aluminum nitrate reverse microemulsion was obtained. Ammonia (AR) was slowly added to the other part of the mixture to prepare an ammonia reverse microemulsion. The ammonia reverse microemulsion was slowly added to the aluminum nitrate reverse microemulsion under stirring to pH = 8.5. Then the precipitates were filtered, dried at 100 ℃ for 12 h, heated to 800 ℃ at 15 ℃/min in an electric furnace, and calcined in air at 800 ℃ for 4 h.

The second step was the preparation of the supported CeO_2-ZrO_2 (Ce∶Zr = 1∶1) solid solution. An aqueous solution of cerium nitrate and zirconium nitrate was dropped into a mixed solution of polyethylene glycol octylphenyl ether (as surfactant), cyclohexane (as oil phase), and 1-hexanol (as co-surfactant) to obtain the reverse microemulsions of the salts. The ammonia/H_2O_2 reverse microemulsion was obtained by dropping ammonia and H_2O_2 into the mixture of polyethylene glycol octylphenyl ether, cyclohexane, and 1-hexanol. The salts and ammonia/H_2O_2 reverse microemulsion were dropped synchronously into a flask with the prepared Si-modified alumina. This mixture was stirred for 1 h, and the precipitate was filtered, dried at 100 ℃ for 12 h, and then calcined at 900−1 100 ℃ for 6−10 h. The samples prepared were denoted xCe-Zr-O/Si-Al_2O_3, where x represented the mass content of CeO_2-ZrO_2 solid solution. The mass content of Si in Si-Al_2O_3 was controlled at 5.2%.

Supported Pd catalyst was prepared by an impregnation method. Weighed $PdCl_2$ was dissolved in a nitric acid aqueous solution, and then the support (20−40 mesh) was added into this Pd-containing so-

lution under ultrasonic treatment. After being dried in vacuum, the supported catalyst was calcined in air at 550 ℃ for 5 h. The Pd loading was 0.2% (mass fraction).

1.2 Catalyst characterization

The BET surface area and pore diameter distribution of the samples were measured at −196 ℃ by nitrogen adsorption on a Micromeritics ASAP 2020 Sorptometer using static adsorption. The X-ray diffraction (XRD) patterns were recorded on a Rigaku D/max-2550/PC diffractometer operated at 50 kV and 180 mA with Cu K_α radiation (λ = 0.154 056 nm). The Raman spectra of samples were obtained on a LabRam-1B spectrometer of Dilor Company, and 632.8 nm line of He-Ne was used. The X-ray photoelectron spectroscopy (XPS) was performed on a Thermo ESCALAB 250 spectrometer using monochromatic Al K_α ($h\nu$ = 486.6 eV). Electrostatic surface charging was observed in all investigated samples owing to their poor electric conductivity. The binding energy (BE) of adventitious C 1*s* (284.8 eV) was used as a reference.

Temperature-programmed reduction (TPR) of the samples was carried out in a conventional flow system equipped with a thermal conductivity detector (TCD). The sample was pretreated in N_2 at 500 ℃ for 1 h before the TPR run. The composition of the reduction gas was 8% H_2/N_2 (25 ml/min) and the heating rate was 600 ℃/h. The amount of hydrogen consumption was quantified by the integration of all the reduction peaks. The reduction degree was defined as the ratio of $Ce^{3+}/(Ce^{4+}+Ce^{3+})$. Oxygen release and reduction degree were derived from hydrogen consumption according to the reaction equation of $CeO_2 + H_2 = 1/2Ce_2O_3 + H_2O$.

The catalyst activity was tested in a fixed bed with a quartz glass reactor packed with 0.1 g catalyst (20−40 mesh). The feed gas consisted of 2% CH_4-90% N_2-8% O_2 (volume) and GHSV was 48 000 h^{-1}. The reaction gas was analyzed by gas chromatograph (GC) with a TCD detector.

2 Results and Discussion

2.1 BET surface area of the samples

The BET surface areas of Ce-Zr-O/Si-Al_2O_3 and the mechanical mixture of CeO_2-ZrO_2 and Si-Al_2O_3 (Ce-Zr-O + Si-Al_2O_3) are listed in Table 1. For the samples calcined at 900−1 000 ℃ for 6 h, the surface area of Ce-Zr-O/Si-Al_2O_3 was larger than that of Si-Al_2O_3 and much larger than that of Ce-Zr-O + Si-Al_2O_3. The surface area of Ce-Zr-O/Si-Al_2O_3 reached a maximum value when the amount of Ce-Zr-O on Si-Al_2O_3 was 10%−15%. For the Ce-Zr-O/Si-Al_2O_3 samples calcined at 1 100 ℃ for 10 h, the surface area decreased obviously with an increase in the CeO_2-ZrO_2 content and was much lower than that of Ce-Zr-O + Si-Al_2O_3. When the content of CeO_2-ZrO_2 was 32.5%, its surface area was only 73 m^2/g, which was still higher than that (38 m^2/g) of the sample prepared by other researchers[25] after being calcined at 1 100 ℃.

The above results showed that there is an interaction between CeO_2-ZrO_2 and Si-Al_2O_3, which resulted in an increase in thermal stability and surface area of Al_2O_3 calcined at 900−1 000 ℃. The most appropriate content of CeO_2-ZrO_2 on Si-Al_2O_3 was 10%−15%. After calcination at 1 100 ℃, the interaction between CeO_2-ZrO_2 and Si-Al_2O_3 may disappear. The presence of CeO_2-ZrO_2 led to the loss of surface area and decrease in thermal stability of Si-Al_2O_3.

2.2 Structure analyses of the samples by XRD and Raman spectroscopy

The XRD patterns in Fig 1 show that for all the Ce-Zr-O/Si-Al_2O_3 and Ce-Zr-O samples calcined at

Table 1　BET surface areas of Ce-Zr-O/Si-Al_2O_3 samples and mechanical mixtures of CeO_2-ZrO_2 and Si-Al_2O_3 (Ce-Zr-O + Si-Al_2O_3) calcined at 900−1100 ℃ for 6−10 h

w(Ce-Zr-O)/%	A_{BET} of Ce-Zr-O/Si-Al_2O_3 (m^2/g)			A_{BET} of Ce-Zr-O + Si-Al_2O_3 * (m^2/g)		
	900 ℃/6 h	1000 ℃/6 h	1100 ℃/10 h	900 ℃/6 h	1000 ℃/6 h	1100 ℃/10 h
0	230	212	174			
10	246	228	130	210	192	157
15	244	241	115	200	183	148
20	237	218	83	190	173	139
25	239	215	87	180	161	131
32.5	237	184	73	165	149	118
100	29	17	1			

* $A_{BET} = A_{BET}(CeO_2\text{-}ZrO_2) \times w(CeO_2\text{-}ZrO_2) + A_{BET}(Si\text{-}Al_2O_3) \times w(Si\text{-}Al_2O_3)$.

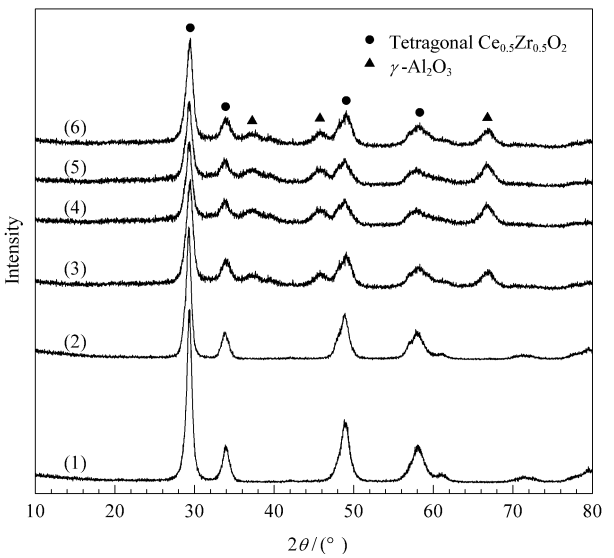

Fig 1 XRD patterns of Ce-Zr-O calcined at 900 ℃ for 6 h (1) and 1000 ℃ for 6 h (2), and Ce-Zr-O/Si-Al_2O_3 calcined at 1000 ℃ for 6 h with Ce-Zr-O contents of 10% (3), 15% (4), 20% (5), and 32.5% (6)

1 000 ℃ for 6 h, there are the diffraction peaks of a single phase tetragonal $Ce_{0.5}Zr_{0.5}O_2$. The diffraction peaks of γ-alumina in the XRD patterns of the Ce-Zr-O/Si-Al_2O_3 samples are weaker. This means that the interaction between CeO_2-ZrO_2 and Al_2O_3 did not change the crystalline phase of both CeO_2-ZrO_2 and Al_2O_3 but improved their thermal stability.

The XRD patterns in Fig 2 show that the X-ray diffraction peaks of 10% Ce-Zr-O/Si-Al_2O_3 calcined at 900 ℃ were the same as that of the sample calcined at 1 000 ℃, which indicate that its structure was unchanged after being calcined at 1 000 ℃. For 10% Ce-Zr-O/Si-Al_2O_3 calcined at 1 100 ℃, a crystalline phase separation of Ce-Zr-O occurred, the diffraction peaks at $2\theta = 28.8°$, 33.4°, 47.9°, and 56.9° can be ascribed to cubic $Ce_{0.75}Zr_{0.25}O_2$ and those at $2\theta = 29.9°$, 34.2°, 34.9°, 49.7°, 50.2°, and 59.6° can be ascribed to tetragonal $Ce_{0.16}Zr_{0.84}O_2$. This is the reason why the presence of Ce-Zr-O led to the loss of surface area and decreased thermal stability of Ce-Zr-O/Si-Al_2O_3.

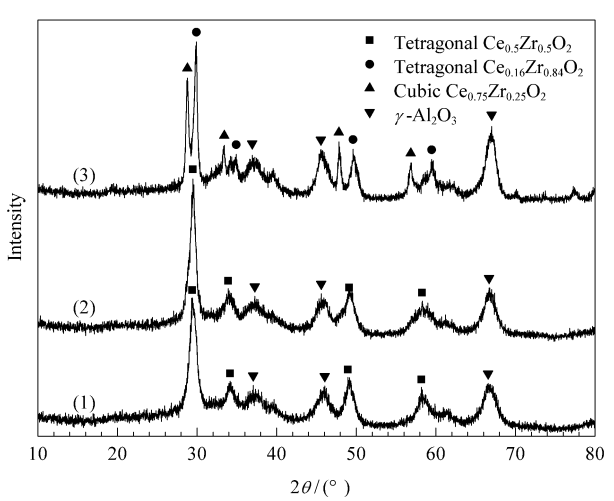

Fig 2 XRD patterns of 10% Ce-Zr-O/Si-Al_2O_3 calcined at 900 ℃ for 6 h (1), 1000 ℃ for 6 h (2), and 1100 ℃ for 10 h (3)

To confirm the type of the crystalline phase in the samples, Raman spectroscopy was used to analyze the structures of 10% Ce-Zr-O/Si-Al_2O_3 and Ce-Zr-O. The results are shown in Fig 3. The results show that the spectrum of 10% Ce-Zr-O/Si-Al_2O_3 calcined at 1 000 ℃ for 6 h was the same as that of Ce-Zr-O calcined at 900 ℃ for 6 h. The four vibration peaks near 630, 470, 310, and 140 cm^{-1} can be ascribed to tetragonal $Ce_{0.5}Zr_{0.5}O_2$ [26], which is consistent with the results obtained by the XRD analysis. For 10% Ce-Zr-O/Si-Al_2O_3 calcined at 1 100 ℃ for 10 h, the vibration peaks near 630, 588, 474, 313, 261, and 142 cm^{-1} can be ascribed to tetragonal $Ce_{0.16}Zr_{0.84}O_2$, and cubic $Ce_{0.75}Zr_{0.25}O_2$ had only one peak near 470 cm^{-1}, which almost overlapped the peak of $Ce_{0.16}Zr_{0.84}O_2$ at 474 cm^{-1}.

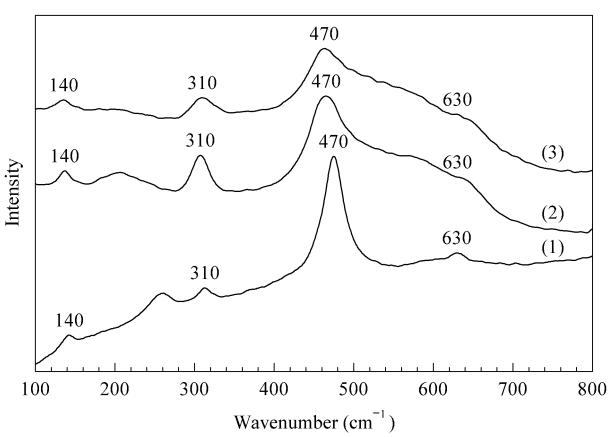

Fig 3 Raman spectra of 10% Ce-Zr-O/Si-Al_2O_3 calcined at 1100 ℃ for 10 h (1) and 1000 ℃ for 6 h (2), and Ce-Zr-O calcined at 900 ℃ for 6 h (3)

2.3 Measurements of the oxygen release capacity of the samples by TPR

The oxygen release capacity of the sample was studied by H_2-TPR. The TPR spectra of the samples calcined at 1 000 ℃ for 6 h are shown in Fig 4, and the reduction characteristics data derived from these spectra are listed in Table 2. The results show that the reduction peaks of Ce-Zr-O/Si-Al_2O_3 were differ-

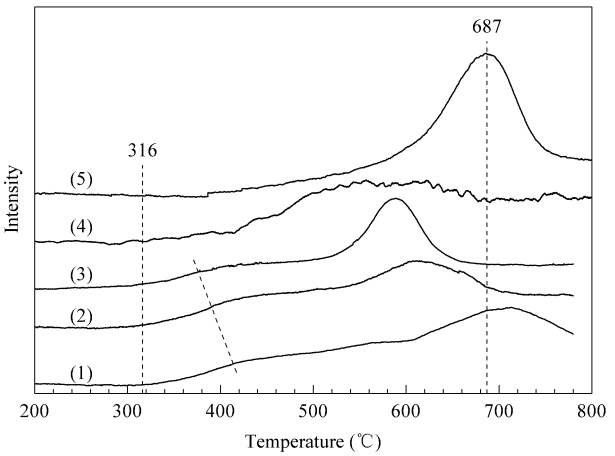

Fig 4　TPR spectra of Ce-Zr-O/Si-Al_2O_3 with Ce-Zr-O contents of 10% (1), 15% (2), 20% (3), and 32.5% (4), and Ce-Zr-O (5) calcined at 1000 ℃ for 6 h

ent from that of CeO_2-ZrO_2. The highest temperature of the reduction peaks decreased much with an increase in the Ce-Zr-O content on Si-Al_2O_3, which indicates that the reduction activity of Ce^{4+} was improved or the oxygen in Ce-Zr-O/Si-Al_2O_3 can be removed at a lower temperature. According to the different reduction temperatures, Ce^{4+} can be classified as surface Ce^{4+} and bulk Ce^{4+}. The former was reduced more easily than the latter. As the surface area of Ce-Zr-O/Si-Al_2O_3 was much larger than that of Ce-Zr-O, the amount of surface Ce^{4+} on Ce-Zr-O/Si-Al_2O_3 should be much more than that of Ce-Zr-O. The amount of surface Ce^{4+} is related to the oxygen storage/release capacity. This was the reason why the peak temperatures of Ce-Zr-O/Si-Al_2O_3 samples were lower than those of Ce-Zr-O. For the Ce-Zr-O/Si-Al_2O_3 samples, the initial temperature of reduction was ~316 ℃, and the first reduction peak was at ~400 ℃.

The results in Table 2 show that the reduction degree, amount of hydrogen consumption, and oxygen release of Ce-Zr-O/Si-Al_2O_3 were much higher than those of Ce-Zr-O, although there were differences in these data between the samples of Ce-Zr-O/Si-Al_2O_3 due to the different amounts of Ce-Zr-O on Si-Al_2O_3. These results indicate that the hydrogen consumption of Ce-Zr-O can be significantly increased after being supported on Si-Al_2O_3, and hydrogen consumption was related to the total oxygen storage capacity.

Table 2　Reduction properties of Ce-Zr-O/Si-Al_2O_3 calcined at 1000 ℃ for 6 h

Sample	Reduction degree (%)	Hydrogen consumption (mmol/mol)	Oxygen release (mmol/mol)
10% Ce-Zr-O/Si-Al_2O_3	96	480	240
15% Ce-Zr-O/Si-Al_2O_3	92	460	230
20% Ce-Zr-O/Si-Al_2O_3	86	430	215
32.5% Ce-Zr-O/Si-Al_2O_3	76	380	195
Ce-Zr-O	61	305	152

2.4　Performance of the catalysts for methane combustion

Fig 5 shows the catalytic activity of 0.2% Pd/Ce-Zr-O/Si-Al_2O_3 for methane combustion. T_{10} (reaction temperature of 10% methane conversion), T_{50}, and T_{90} were 350, 400, and 480 ℃, respectively. However, the catalytic activity was almost unchanged with the different amounts of the CeO_2-ZrO_2 solid solution. Based on the larger surface area of 10% Ce-Zr-O/Si-Al_2O_3, it was chosen as the support of the supported Pd catalyst for methane combustion.

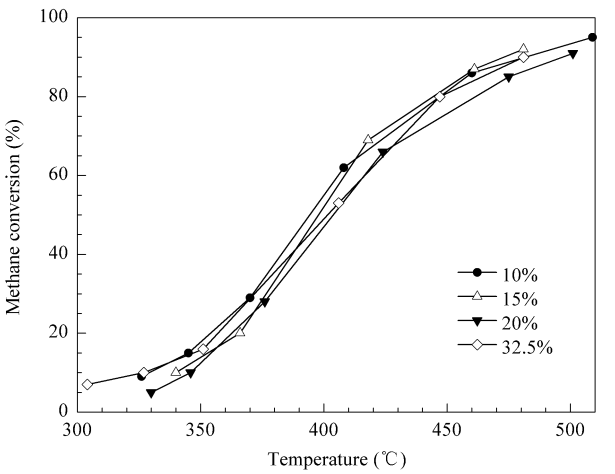

Fig 5　Effect of Ce-Zr-O content on the performance of Pd/Ce-Zr-O/Si-Al_2O_3 (Ce-Zr-O/Si-Al_2O_3 was calcined at 1000 ℃ for 6 h, and the catalyst was calcined at 550 ℃ for 5 h)

The effects of the calcination condition of the carrier on the performance of Pd catalysts for methane combustion are shown in Fig 6. It can be seen that Pd supported on 10% Ce-Zr-O/Si-Al_2O_3 calcined at 1 000 ℃ for 6 h had higher catalytic activity, that is, 1 000 ℃ is a suitable condition of calcination for 10% Ce-Zr-O/Si-Al_2O_3. This is because a higher calcination temperature (such as 1 100 ℃) can lead to the loss of surface area, separation of the Ce-Zr-O crystalline phase, and disappearance of the interaction between Ce-Zr-O and Si-Al_2O_3. A lower calcination temperature cannot endow enough stability to the support, resulting in a decrease of the structure sta-

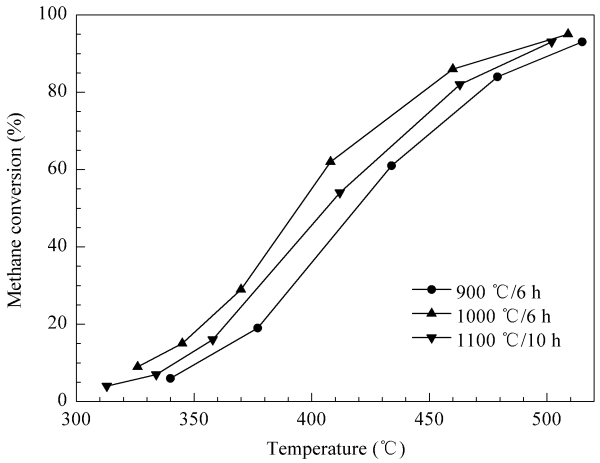

Fig 6 Effect of calcination conditions of 10% Ce-Zr-O/Si-Al_2O_3 on methane conversion over Pd/10% Ce-Zr-O/Si-Al_2O_3 calcined at 550 ℃ for 5 h

bility of the Pd catalyst and the Pd dispersion on the support[23].

Fig 7 shows the catalytic performance of Pd/10% Ce-Zr-O/Si-Al_2O_3 unreduced and pre-reduced by H_2 at 450 ℃ for 1 h for methane combustion. The results show that the reduction treatment of the catalyst before use can improve its catalytic activity. T_{90} over the pre-reduced Pd/10% Ce-Zr-O/Si-Al_2O_3 catalyst was only 350 ℃, which was 130 ℃ lower than that over the unreduced catalyst.

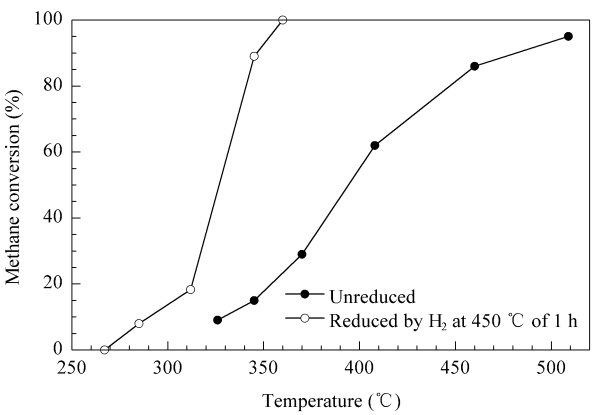

Fig 7 Effect of H_2 pre-reduction on the performance of the Pd/10% Ce-Zr-O/Si-Al_2O_3 catalyst

To study the effect of the carrier on the catalytic performance of Pd catalyst for methane combustion, 10% Ce-Zr-O/Si-Al_2O_3, Ce-Zr-O, Si-Al_2O_3, and a mechanical mixture of 10% Ce-Zr-O and Si-Al_2O_3 were used as the support. Their catalytic performance for methane combustion is shown in Fig 8. They were pre-reduced by H_2 at 450 ℃ for 1 h. The results show that the catalytic activity decreased in the order

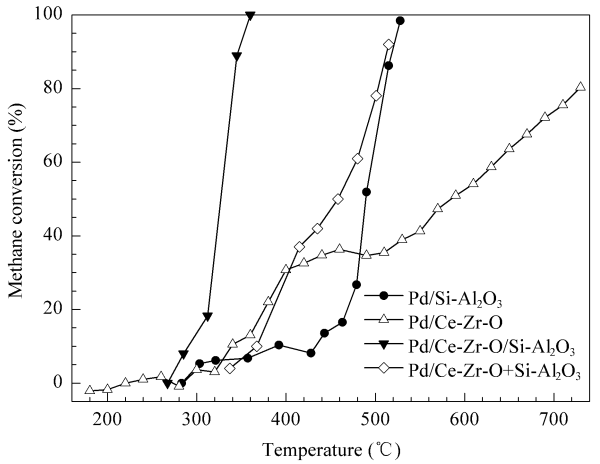

Fig 8 Methane conversion as a function of the reaction temperature over the reduced catalysts

Pd/10% Ce-Zr-O/Si-Al_2O_3 > Pd/(10% Ce-Zr-O + Si-Al_2O_3) > Pd/Si-Al_2O_3 > Pd/Ce-Zr-O.

The results exhibit that as the support of Pd catalysts for methane combustion, 10% Ce-Zr-O/Si-Al_2O_3 was the best because it possessed good oxygen storage properties of CeO_2-ZrO_2 solid solution and larger surface area of Al_2O_3, and also a much higher thermal stability due to the interaction between CeO_2-ZrO_2 and Al_2O_3. For the Pd/10% Ce-Zr-O/Si-Al_2O_3 catalyst, the reduced sample had higher activity for methane combustion based on the existence of $Pd^{\delta+}$ ($1<\delta^+<2$) or the co-existence of Pd^0/PdO on the support.

2.5 Studies of chemical states of the active sites by XPS

In order to understand the chemical states of the active sites on the catalysts, Pd/10% Ce-Zr-O/Si-Al_2O_3 and Pd/Ce-Zr-O were studied by XPS before and after reduction. The results are shown in Fig 9. The bands at 332.8–333.1 eV can be assigned to Zr $3p_{1/2}$ and the bands at 346.4–346.9 eV can be assigned to Zr $3p_{3/2}$[27].

The Pd $3d$ bands were overlapped partly by that of Zr $3p$, and the valence states of palladium were different in the four samples. For unreduced Pd/Ce-Zr-O and Pd/Ce-Zr-O/Si-Al_2O_3, the bands located at 337.0 (337.1) and 342.7 (342.6) eV were similar to that of Pd^{2+} in palladium chloride[27]. For reduced Pd/Ce-Zr-O, the bands at 337.3 and 342.9 eV were also similar to those of Pd^{2+} in palladium chloride, and the bands at 335.4 and 341.6 eV can be assigned to Pd^0[27], which indicates that some Pd^{2+} was reduced to Pd^0. For reduced Pd/Ce-Zr-O/Si-Al_2O_3,

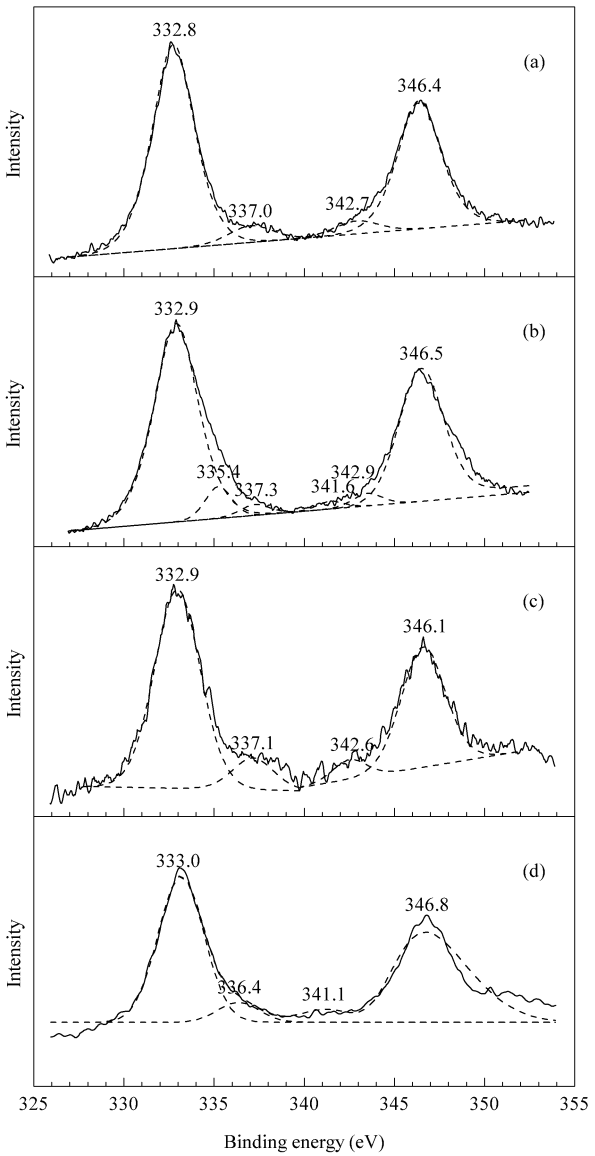

Fig 9　Zr 3*p* and Pd 3*d* XPS spectra of Pd/Ce-Zr-O (a), reduced Pd/Ce-Zr-O (b), Pd/10% Ce-Zr-O/Si-Al_2O_3 (c), and reduced Pd/10% Ce-Zr-O/Si-Al_2O_3 (d)

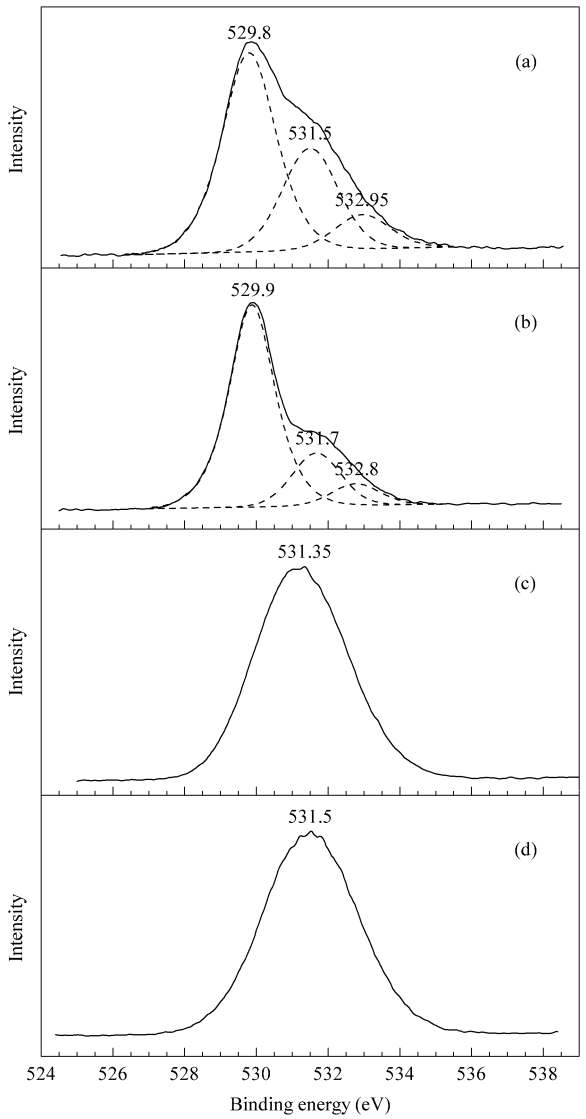

Fig 10　O 1*s* XPS spectra of Pd/Ce-Zr-O (a), reduced Pd/Ce-Zr-O (b), Pd/10% Ce-Zr-O/Si-Al_2O_3 (c), and reduced Pd/10% Ce-Zr-O/Si-Al_2O_3 (d)

the bands at 336.4 and 341.1 eV were similar to that of Pd in Pd_3Si[27], and its valence state was between +1 and +2.

The O 1*s* XPS spectra in Fig 10 indicate that there were mainly 3 kinds of oxygen on the unreduced and reduced Pd/Ce-Zr-O catalysts. Their bands were located at 529.8, 531.6, and 532.9 eV, which can be assigned to bulk oxygen, surface oxygen, and adsorbed oxygen, respectively. After reduction by H_2, the O 1*s* bands at 531.6 and 532.9 eV of Pd/Ce-Zr-O weakened obviously, that is, surface and adsorbed oxygen was partly removed. For Pd/Ce-Zr-O/Si-Al_2O_3, on both the reduced or unreduced catalyst, only one band at 531.4 eV was observed, which showed that there was almost no difference between the three kinds of oxygen species on Pd/Ce-Zr-O/Si-Al_2O_3, resulting in that the oxygen properties of Pd/Ce-Zr-O/Si-Al_2O_3 was hardly changed after being reduced. Compared with the Pd/Ce-Zr-O catalyst, the oxygen on Pd/Ce-Zr-O/Si-Al_2O_3 was more easily removed, which is similar to the surface oxygen on Pd/Ce-Zr-O. This is one of the reasons why Pd/Ce-Zr-O/Si-Al_2O_3 has higher catalytic activity than Pd/Ce-Zr-O for methane combustion.

The XPS results above show that the support properties affect the reduction of Pd active sites, and the difference between Ce-Zr-O and Ce-Zr-O/Si-

Al_2O_3 may be due to the difference in their oxygen storage/release capacity.

3 Conclusions

A Ce-Zr-O/Si-Al_2O_3 support material with better properties has been prepared by the reverse microemulsion method. The crystalline phase of CeO_2-ZrO_2 on Si-Al_2O_3 was the same as that of unsupported CeO_2-ZrO_2. The interaction between CeO_2-ZrO_2 and Si-Al_2O_3 resulted in an increase in thermal stability and surface area of Ce-Zr-O/Si-Al_2O_3 such that it can be used up to 1 000 ℃, and an obvious improvement in the oxygen storage/release capacity of the catalyst. The appropriate content of CeO_2-ZrO_2 on Si-Al_2O_3 was 10%–15%. As the support of a Pd catalyst for methane combustion, Ce-Zr-O/Si-Al_2O_3 had better properties than Ce-Zr-O, Si-Al_2O_3, and a mixture of Ce-Zr-O + Si-Al_2O_3. With the 0.2% Pd/10% Ce-Zr-O/Si-Al_2O_3 catalyst, T_{90} was only 345 ℃, which is 175 ℃ lower than that of Pd supported on other supports.

References

1 Horiuchi T, Osaki T, Sugiyama T, Masuda H, Horio M, Suzuki K, Mori T, Sago T. *J Chem Soc, Faraday Trans*, 1994, **90**(17): 2573

2 Fernández-García M, Martínez-Arias A, Iglesias-Juez A, Hungría A B, Anderson J A, Conesa J C, Soria J. *Appl Catal B*, 2001, **31**(1): 39

3 González-Velasco J R, Gutiérrez-Ortiz M A, Marc J-L, Botas J A, González-Marcos M P, Blanchard G. *Appl Catal B*, 1999, **22**(3): 167

4 Pérez-Osorio G, Castillón F, Simakov A, Tiznado H, Zaera F, Fuentes S. *Appl Catal B*, 2007, **69**(3-4): 219

5 Yue B H, Zhou R X, Wang Y J, Zheng X M. *J Mol Catal A*, 2005, **238**(1-2): 241

6 Rossignol S, Kappenstein C. *Int J Inorg Mater*, 2001, **3**(1): 51

7 Praserthdam P, Inoue M, Mekasuvandumrong O, Thanakulrangsan W, Phatanasri S. *Inorg Chem Commun*, 2000, **3**(11): 671

8 Horiuchi T, Chen L, Osaki T, Sugiyama T, Suzuki K, Mori T. *Catal Lett*, 1999, **58**(2-3): 89

9 Horiuchi T, Osaki T, Sugiyama T, Suzuki K, Mori T. *J Non-Cryst Solids*, 2001, **291**(3): 187

10 Shigapov A N, Graham G W, McCabe R W, Plummer H K Jr. *Appl Catal A*, 2001, **210**(1-2): 287

11 Inoue M, Kominami H, Inui T. *J Am Ceram Soc*, 1992, **75**(9): 2597

12 Inoue M, Tanino H, Kondo Y, Inui T. *J Am Ceram Soc*, 1989, **72**(2): 352

13 Zarur A J, Hwu H H, Ying J Y. *Langmuir*, 2000, **16**(7): 3042

14 Ozawa M. *J Alloy Compd*, 1998, **275-277**: 886

15 Gandhi H S, Shelef M. *Stud Surf Sci Catal*, 1987, **30**: 199

16 Kim G. *Ind Eng Chem, Prod Res Dev*, 1982, **21**(2): 267

17 Suhonen S, Valden M, Hietikko M, Laitinen R, Savimäki A, Härkönen M. *Appl Catal A*, 2001, **218**(1-2): 151

18 Schulz H, Stark W J, Maciejewski M, Pratsinis S E, Baiker A. *J Mater Chem*, 2003, **13**(12): 2979

19 Fernández-García M, Martínez-Arias A, Guerrero-Ruiz A, Conesa J C, Soria J. *J Catal*, 2002, **211**(2): 326

20 Chen M, Zhang P Zh, Zheng X M. *Catal Today*, 2004, **93-95**: 671

21 Wang X H, Lu G Zh, Guo Y, Wang Y S, Guo Y L. *Mater Chem Phys*, 2005, **90**(2-3): 225

22 Wang X H, Guo Y, Lu G Zh, Guo Y L, Wang Y S, Zhang Zh G, Liu X H. *J Rare Earths*, 2004, **22**(6): 763

23 Wang X H, Guo Y, Lu G Zh, Hu Y, Jiang L Zh, Guo Y L, Zhang Zh G. *Catal Today*, 2007, **126**(3-4): 369

24 Wang X H, Lu G Zh, Guo Y, Xue Y Y, Jiang L Zh, Guo Y L, Zhang Zh G. *Catal Today*, 2007, **126**(3-4): 412

25 Fernández-García M, Martínez-Arias A, Hungría A B, Iglesias-Juez A, Conesa J C, Soria J. *Phys Chem Chem Phys*, 2002, **4**(11): 2473

26 Kim D J, Jung H J. *J Am Ceram Soc*, 1993, **76**(8): 2106

27 Moulder J F, Stickle W F, Sobol P E, Domben K D. Handbook of X-Ray Photoelectron Spectroscopy. Eden Prairie: Perkin-Elmer Corporation, Physical Electronics Division, 1993. 108, 119